

Temperature tuning of BaGa₄Se₇ optical parametric oscillator

Hui Kong (孔辉)^{1,2}, Jintian Bian (卞进田)^{1,2*}, Jiyong Yao (姚吉勇)³, Qing Ye (叶庆)^{1,2}, and Xiaoquan Sun (孙晓泉)^{1,2**}

¹State Key Laboratory of Pulsed Power Laser Technology, National University of Defense Technology, Hefei 230037, China

²Advanced Laser Technology Laboratory of Anhui Province, Hefei 230037, China

³Technical Institute of Physics and Chemistry, Chinese Academy of Sciences, Beijing 100190, China

*Corresponding author: bianjt@126.com

**Corresponding author: sun_xq@nudt.edu.cn

Received June 14, 2020 | Accepted September 11, 2020 | Posted Online December 3, 2020

The temperature tuning of BaGa₄Se₇ (BGSe) was demonstrated for the first time, to the best of our knowledge. When the temperature of BGSe (56.3°) was raised from 30°C to 140°C, the idler light under type I raised from 3637 nm to 3989 nm, the tunable range reached 352 nm, and $\Delta\lambda_2/\Delta T$ reached 3.20 nm/°C. We calculated the phase matching curve of BGSe when θ and T took different values. The relationship between θ and $\Delta\lambda_2/\Delta T$ was obtained by fixing θ at 0°. The maximum $\Delta\lambda_2/\Delta T$ and its corresponding (θ, \varnothing) phase matching type were reported under different fixed λ_2 (3 μm , 3.2 μm , . . . , 5 μm).

Keywords: temperature tuning; BaGa₄Se₇; optical parametric oscillator.

DOI: [10.3788/COL202119.021901](https://doi.org/10.3788/COL202119.021901)

1. Introduction

The mid-infrared (IR) coherent sources in the 3–5 μm range have always been intensively desired for a wide range of scientific and technological applications in remote sensing, spectrum analysis, materials diagnostics, aerospace fields, etc.^[1]. Optical parametric oscillation is an attractive approach, especially when high energy and average power are demanded simultaneously^[2,3]. BaGa₄Se₇ (BGSe) showed excellent optical quality and performance in a 1.064 μm pumped nanosecond optical parametric oscillator (OPO). Its second harmonic generation (SHG) effect is about 2–3 times that of the benchmark material AgGaS₂, and the surface laser damage threshold is about 3.7 times that of AgGaS₂. The transparent range of this crystal covers 0.47 to 18 μm , which makes it possible to obtain mid-IR coherent light through parametric down-conversion from 1 μm (Nd and Yb) lasers^[4].

In 2010, the BGSe crystal was synthesized for the first time^[4], to the best of our knowledge, and the thermal conductivity coefficients and laser damage threshold were measured in 2012^[5]. In 2013, Yang *et al.* demonstrated a mid-IR optical parametric amplifier with BGSe pumped by a 1064 nm Nd:Y₃Al₅O₁₂ (Nd:YAG) laser. A maximum idler output of 830 μJ at 3.9 μm was obtained at pump energy of ~ 9.1 mJ, and 3–5 μm idler tuning range was demonstrated for the first time, to the best of our knowledge, through angle tuning^[6]. In 2016, Kostyukova *et al.* achieved the unprecedented tuning capability from 2.7 to 17 μm with a single crystal cut by angle tuning^[7]. But up to now, we have not seen the report of temperature tuning of a BGSe OPO.

Angle tuning has many advantages, such as wide tuning range and continuously tunable wavelength. However, it is necessary to use a precise rotating table to control the crystal rotation angle, and the pump efficiency decreases as the tunable angles increase due to the crystal's reflection. Temperature tuning uses a temperature control furnace to change the wavelength of idler light by adjusting the temperature of the crystal. Generally, the tuning range of temperature tuning is smaller than that of angle tuning. But, the mechanical structure is stable, and the idler energy is stable for its vertical incidence, so it can be used on many occasions such as vehicle, ship, and airborne applications. In 2017, Zhai *et al.* measured the principal axis refractive index n_x , n_y , n_z of BGSe crystal at different temperatures (25°C–150°C) and gave the relationship between the principal thermal refractive index and temperature dn_x/dT , dn_y/dT , dn_z/dT in the wavelength range of $0.254 \mu\text{m} \leq \lambda \leq 2.325 \mu\text{m}$ ^[8]. In 2018, Kato *et al.* measured the fundamental wavelength of the crystal to achieve the maximum SHG efficiency at different temperatures and gave the dn_x/dT , dn_y/dT , dn_z/dT of the crystal in a larger wavelength range ($0.901 \mu\text{m} \leq \lambda \leq 10.5910 \mu\text{m}$)^[9]. These works provided important theoretical guidance for the temperature tuning of BGSe OPOs. Therefore, based on the Sellmeier equation in Ref. [9], we first calculated the phase matching curves of BGSe under type I and type II at different temperatures. Then, we obtained the relationship between θ and $\Delta\lambda_2/\Delta T$ with fixed $\varnothing = 0^\circ$. Next, the maximum $\Delta\lambda_2/\Delta T$ and its corresponding (θ, \varnothing) phase matching type were reported with fixed $\lambda_2 = 3 \mu\text{m}$, 3.2 μm , 3.4 μm , . . . , 5 μm . In addition,

temperature tuning of BGSe ($56.3^\circ, 0^\circ$) was demonstrated. The wavelength tuning of 3637–3989 nm was realized with the temperature tunable from 30°C to 140°C , corresponding to $\Delta\lambda_2/\Delta T = 3.2 \text{ nm}/^\circ\text{C}$. In 2020, six periodically poled lithium niobate (PPLN) crystals were used by Niu *et al.* to achieve a wide range tuning of 2.2–4.8 μm from 25°C to 200°C ^[10], where the tunable range was approximately 3000–3375 nm when the grating period was 30 μm , corresponding to $\Delta\lambda_2/\Delta T \approx 2.14 \text{ nm}/^\circ\text{C}$ under λ_2 of 3000 nm. The results show that the $\Delta\lambda_2/\Delta T$ of the BGSe crystal is larger than that of the PPLN crystal. In addition, the BGSe crystal also has wide transmission range and angle tuning ability. The combination of temperature tuning and angle tuning has great development potential.

2. Methods

2.1 Phase matching curve at room temperature

Up to now, four articles^[11–14] have given the Sellmeier equation of BGSe at room temperature. We select the equation in Ref. [14] to calculate the phase matching curve of BGSe at room temperature, with wavelength $0.901 \mu\text{m} \leq \lambda \leq 10.5910 \mu\text{m}$, as shown in Eq. (1):

$$\begin{cases} n_x^2 = 6.72431 + \frac{0.26375}{\lambda^2 - 0.04248} + \frac{602.97}{\lambda^2 - 749.87} \\ n_y^2 = 6.86603 + \frac{0.26816}{\lambda^2 - 0.04259} + \frac{682.97}{\lambda^2 - 781.78} \\ n_z^2 = 7.16709 + \frac{0.32681}{\lambda^2 - 0.06973} + \frac{731.86}{\lambda^2 - 790.16} \end{cases} \quad (1)$$

The light incident into the BGSe crystal can be represented by (θ, \varnothing) , where θ is the angle between the light and the Z axis of the crystal, and \varnothing is the angle between the kOZ plane and X axis of the crystal. Each light has two refractive indices. The larger one is called slow light $n_{e_1}(\theta, \varnothing)$, and the smaller one is called fast light $n_{e_2}(\theta, \varnothing)$. The $n_{e_1}(\theta, \varnothing)$, $n_{e_2}(\theta, \varnothing)$ can be derived from n_i^2 ($i = x, y, z$)^[15].

The pump light λ_3 , signal light λ_1 , and idler light λ_2 should be in accord with Eqs. (2) and (3):

$$\frac{1}{\lambda_3} = \frac{1}{\lambda_1} + \frac{1}{\lambda_2}, \quad (2)$$

$$\frac{n_{e_2}^{\lambda_3}}{\lambda_3} = \frac{n_{e_1}^{\lambda_1}}{\lambda_1} + \frac{n_{e_1}^{\lambda_2}}{\lambda_2} \text{ (I), or } \frac{n_{e_2}^{\lambda_3}}{\lambda_3} = \frac{n_{e_1}^{\lambda_1}}{\lambda_1} + \frac{n_{e_2}^{\lambda_2}}{\lambda_2} \text{ (II-A), or}$$

$$\frac{n_{e_2}^{\lambda_3}}{\lambda_3} = \frac{n_{e_1}^{\lambda_1}}{\lambda_1} + \frac{n_{e_2}^{\lambda_2}}{\lambda_2} \text{ (II-B),} \quad (3)$$

where $n_{e_2}^{\lambda_3}$ is the refractive index of fast light at λ_3 ; $n_{e_1}^{\lambda_1}$ and $n_{e_2}^{\lambda_1}$ are the refractive indices of slow light and fast light at λ_i ($i = 1, 2$). The phase matching curves of BGSe at room temperature can be calculated from Eqs. (1)–(3).

The λ_3 was set to 1064 nm, and the sampling accuracy of λ_2 was set to 1 nm. Since BGSe is a biaxial crystal, the refractive index is related to (θ, \varnothing) . We investigated the relationship between θ and λ_2 , λ_1 when $\varnothing = 0^\circ, 10^\circ, 20^\circ, \dots, 90^\circ$. Because BGSe has no suitable matching angles under type II-A phase

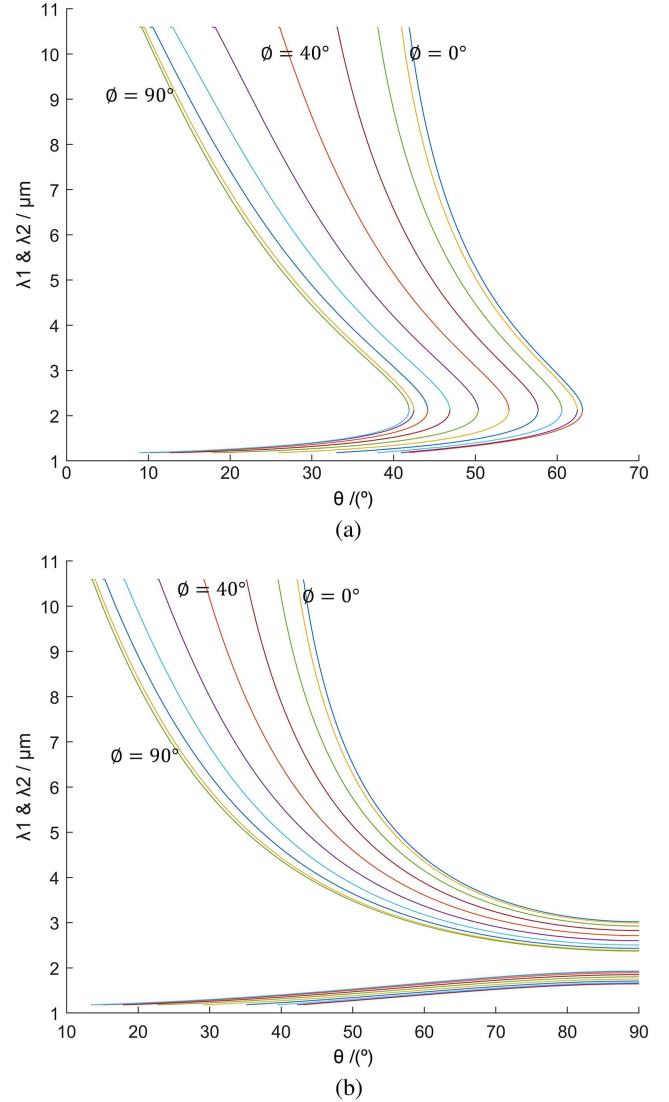


Fig. 1. Phase matching curves of BGSe at room temperature under (a) type I and (b) type II-B conditions ($\lambda_3 = 1064 \text{ nm}$).

matching condition, we only give the phase matching curves of type I and type II-B, which are shown in Fig. 1.

As shown in Fig. 1, when \varnothing rises from 0° to 90° , the curves of type I move from right to left, and the upper curves of type II-B move from right to left, too. The changes of the phase matching curve are tiny when \varnothing is 0° – 10° and 80° – 90° .

2.2 Phase matching curve at 20°C – 140°C

The refractive index of BGSe at 20°C – 140°C can be revised from Eqs. (4) and (5) with wavelength $0.901 \mu\text{m} \leq \lambda \leq 10.5910 \mu\text{m}$ ^[9]:

$$\begin{cases} \frac{dn_x}{dT} = \left(\frac{6.0868}{\lambda^3} - \frac{12.6368}{\lambda^2} + \frac{10.5624}{\lambda} + 1.9583 \right) \times 10^{-5} (^\circ\text{C}^{-1}) \\ \frac{dn_y}{dT} = \left(\frac{6.3935}{\lambda^3} - \frac{13.1762}{\lambda^2} + \frac{10.8950}{\lambda} + 2.4079 \right) \times 10^{-5} (^\circ\text{C}^{-1}), \\ \frac{dn_z}{dT} = \left(\frac{6.3141}{\lambda^3} - \frac{13.0790}{\lambda^2} + \frac{10.8486}{\lambda} + 2.0758 \right) \times 10^{-5} (^\circ\text{C}^{-1}) \end{cases} \quad (4)$$

$$n_i(T) = n_i + \frac{dn_i}{dT}(T - T_0), \quad (5)$$

where $n_i(T)$ and n_i ($i = x, y, z$) are the refractive indices at T and 20°C on the dielectric frame (x, y, z) . The phase matching curve at 20°C – 140°C can be derived from Eqs. (1)–(5).

Due to the effective nonlinear coefficient being large when $\varnothing = 0^\circ$ under type I and $\varnothing = 20^\circ$ under type II-B^[16], we only give the phase matching curve of BGSe crystal at $T = 20^\circ\text{C}$, 80°C , 140°C with $\varnothing = 0^\circ$ and $\varnothing = 20^\circ$, which is shown in Fig. 2.

As shown in Fig. 2, when the temperature is raised from 20°C to 140°C , the curves of type I move from left to right, and the upper curves of type II-B move from left to right, too, so the wavelength of idler light increases as the temperature rises.

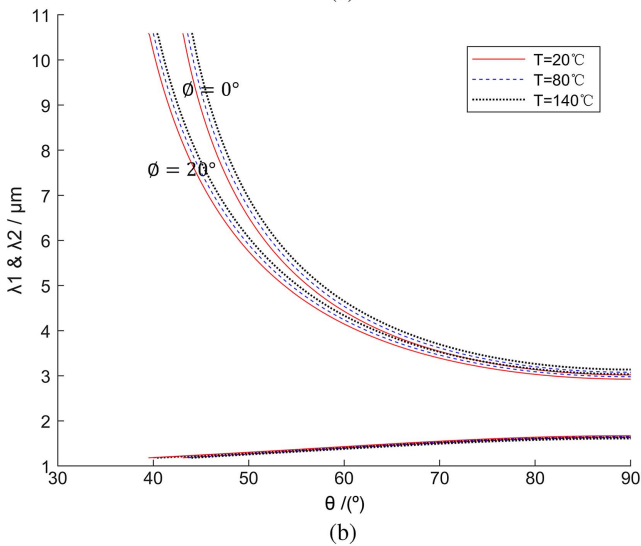
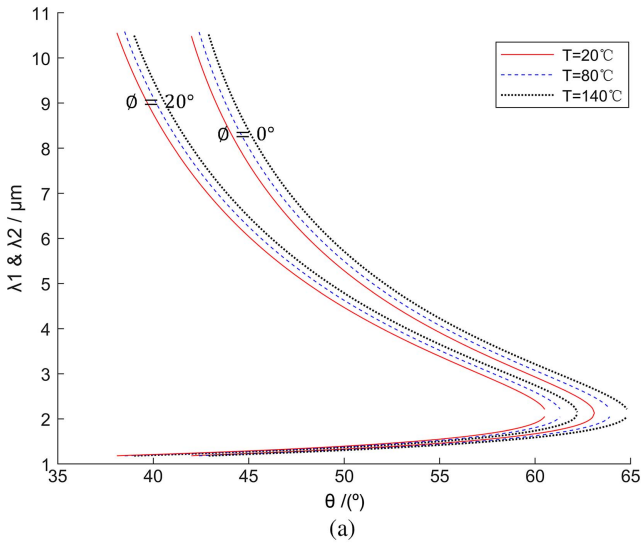


Fig. 2. Phase matching curve at 20°C , 80°C , and 140°C under (a) type I and (b) type II-B conditions ($\lambda_3 = 1064 \text{ nm}$, $\varnothing = 0^\circ, 20^\circ$).

2.3 Relationship between $\Delta\lambda_2/\Delta T$ and θ when $\varnothing = 0^\circ$

The $\Delta\lambda_2/\Delta T$ varied when (θ, \varnothing) changed. The relationship between $\Delta\lambda_2/\Delta T$ and θ when $\varnothing = 0^\circ$ is shown in Fig. 3, and the corresponding wavelength of idler light at $T = 20^\circ\text{C}$ is obtained.

As shown in Fig. 3, the $\Delta\lambda_2/\Delta T$ are not given when $\varnothing = 0^\circ$, $\theta \geq 65^\circ$ under type I because they don't meet the phase matching condition. The maximum value of $\Delta\lambda_2/\Delta T$ is $6.175 \text{ nm}/^\circ\text{C}$ when $\theta = 45^\circ$ under the type I condition. $\Delta\lambda_2/\Delta T$ and $\lambda(20^\circ\text{C})$ decrease monotonically as θ increases. The maximum value of $\Delta\lambda_2/\Delta T$ is $6.60 \text{ nm}/^\circ\text{C}$ when $\theta = 45^\circ$ under the type II-B condition. $\Delta\lambda_2/\Delta T$ and $\lambda(20^\circ\text{C})$ decrease monotonically as θ increases, too. If the unit of λ changes from nanometers (nm) to cm^{-1} , $\Delta\lambda_2/\Delta T$ is very close, which is from the minimum $0.76 \text{ cm}^{-1}/^\circ\text{C}$ to the maximum $2.52 \text{ cm}^{-1}/^\circ\text{C}$. $\Delta\lambda_2/\Delta T$ of type II-B is larger than that of type I when $\theta = 45^\circ$, while $\Delta\lambda_2/\Delta T$ of type I is larger than that of type II-B at other points.

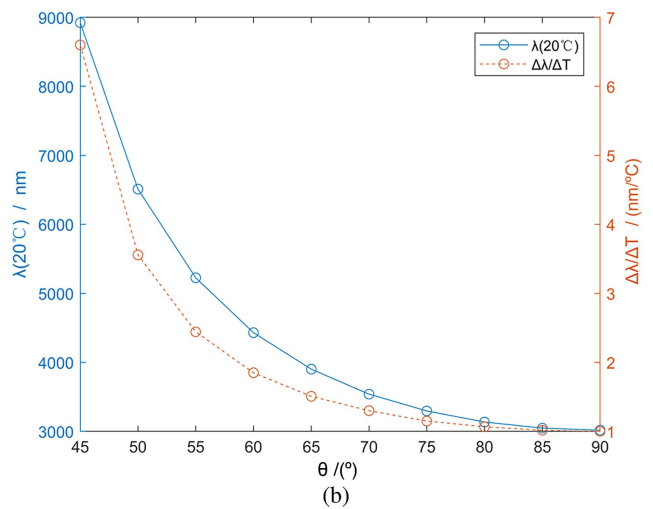
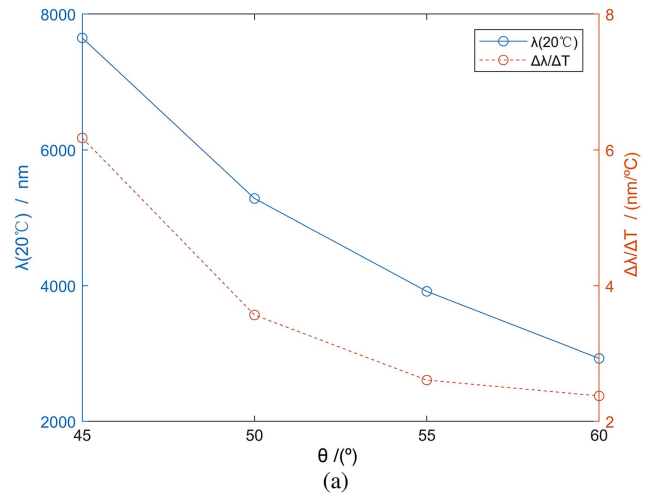


Fig. 3. Wavelength of idler light at $T = 20^\circ\text{C}$ and $\Delta\lambda_2/\Delta T$ at each θ when $\varnothing = 0^\circ$ under (a) type I and (b) type II-B conditions.

Table 1. Peak of $\Delta\lambda_2/\Delta T$ and Corresponding (θ, \varnothing) , Matching Type When λ_2 Is Fixed.

λ_2 [20°C] [μm]	3	3.2	3.4	3.6	3.8	4	4.2	4.4	4.6	4.8	5	
I	θ [°]	59.5	58.4	57.3	56.4	55.4	54.6	53.6	52.9	52.2	51.5	50.8
	\varnothing [°]	4.1	4.5	5.3	3.4	4.3	1.8	5	3.3	2	1.9	3
	λ_2 [140°C] [μm]	3.28	3.48	3.69	3.90	4.11	4.32	4.53	4.75	4.96	5.18	5.40
	$\Delta\lambda_2/\Delta T$ [nm/°C]	2.36	2.36	2.39	2.47	2.55	2.66	2.77	2.90	3.03	3.18	3.33
II-B	θ [°]	89.3	77.6	72.6	68.8	66.1	63.9	61.9	60.2	58.7	57.4	56.2
	\varnothing [°]	8.5	3.4	1.9	5.9	4.4	1.3	2.6	2.4	2.5	1	1.4
	λ_2 [140°C] [μm]	3.12	3.33	3.55	3.76	3.97	4.19	4.40	4.62	4.84	5.05	5.27
	$\Delta\lambda_2/\Delta T$ [nm/°C]	0.99	1.10	1.21	1.33	1.44	1.57	1.70	1.83	1.97	2.12	2.27

2.4 Peak of $\Delta\lambda_2/\Delta T$ and corresponding (θ, \varnothing) , matching type when λ_2 is fixed

We also give $\Delta\lambda_2/\Delta T$ at each (θ, \varnothing) and matching type when the wavelength of the idler light is fixed. The maximum value of $\Delta\lambda_2/\Delta T$ and the corresponding (θ, \varnothing) , matching type are listed in Table 1 when the wavelength of the idler light is from 3 μm to 5 μm at 20°C. In addition, the idler light of the corresponding (θ, \varnothing) and matching type at 140°C is reported.

As shown in Table 1, $\Delta\lambda_2/\Delta T$ increases monotonically with the increase of λ_2 (20°C). The $\Delta\lambda_2/\Delta T$ of type I is larger than that of type II-B at 3–5 μm , and the \varnothing corresponding to the maximum $\Delta\lambda_2/\Delta T$ is near 0°. For example, when λ_2 (20°C) is 3.6 μm , the $\Delta\lambda_2/\Delta T$ and corresponding (θ, \varnothing) , matching type are shown in Table 2 when \varnothing are close to 0°.

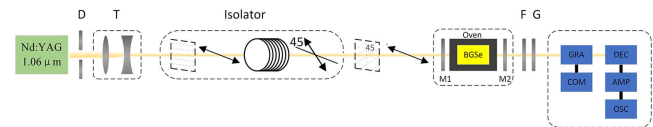
As shown in Table 2, $\Delta\lambda_2/\Delta T$ of $\varnothing = 0^\circ$ is slightly lower compared to the maximum when $\varnothing = 3.4^\circ$. For the convenience of crystal cutting, it is recommended to cut according to $\varnothing = 0^\circ$. The following is the experimental verification of the peak wavelength of BGSe (56.3°, 0°) at different temperatures under the type I phase matching condition.

3. Experimental Setup

The experimental setup is shown in Fig. 4. The BGSe OPO is pumped by an SL800 Series pulsed Nd:YAG along with 13 ns pulse width (FWHM), 8 mm beam diameter, and 1 Hz pulse

Table 2. $\Delta\lambda_2/\Delta T$ When \varnothing Is Close to 0° and λ_2 at 140°C.

θ [°]	56.3	56.4	56.5
\varnothing [°]	5.2	3.4	0
λ_2 [140°C] [nm]	3895	3896	3892
$\Delta\lambda_2/\Delta T$ [nm/°C]	2.458	2.467	2.433

**Fig. 4.** Schematic diagram of the experimental setup.

repetition frequency. A pinhole is placed behind the Nd:YAG for adjusting the light path, and the beam diameter is compressed to 4 mm through a telescope system to improve the energy density of the pump light.

Due to M2 being highly reflective of the pump light, in order to prevent feedback to the Nd:YAG laser, a polarizer and a Faraday rotator were placed after the telescope system to form an optical isolator. Since the polarization direction of the laser output was horizontal, the polarization direction of the polarizer was also adjusted to the horizontal direction. The polarization direction of the pump light rotated 45° to the right after passing the isolator. The BGSe crystal was a 6 mm × 8 mm × 15 mm cuboid with a cutting angle of (56.3°, 0°). Phase matching is satisfied when the pump light is e_2 . The polarization direction of e_2 is perpendicular to the XOZ plane, that is, parallel to the long side of the crystal at 8 mm. In order to make the BGSe crystal horizontally placed on the temperature control furnace and improve the stability of the equipment, it is necessary to use a 45° phase delay plate to rotate the polarization direction 45° to the left again to make the polarization direction return to the horizontal direction.

M1 is highly transmissive (HT) for the pump (P, $T > 95\%$) and highly reflective (HR) for the signal (S, 1.4–1.6 μm , $R > 99\%$). M2 is HR for the pump (P, $R > 99\%$) and the signal (S, 1.4–1.6 μm , $R = 90\%$) and HT for the idler (I, $T > 95\%$). The BGSe crystal was polished but not coated. A copper gripper holds the crystals in a temperature control furnace (HCP TC038-PC) that can tune the temperature up to 200°C, and tunable accuracy is 0.1°C.

A filter and a Ge plate are placed behind M2. The transmittance of the filter is about 1% at 1064 nm and 95%–99% at

3–5 μm . The transmittance of Ge is zero at 1064 nm and about 80% at 3–5 μm .

The idler light was detected by a grating spectrometer (Omni-300 λ , Zolix). The peak wavelength of the blazed grating is 3000 nm, the grating line is 300 g/mm, and the minimum resolution is 1 nm. The computer controls the rotation of the grating to make its transmission wavelength tunable from 2000 nm to 6000 nm, and the adjustment accuracy is 1 nm. The DEC-M204-InSb detector and ZAMP amplifier from Zolix detected and amplified the idler light transmitted from the grating spectrometer. And the idler light energy from ZAMP amplifier was measured by a DSOX3054 oscilloscope. When the maximum energy emerges in the oscilloscope, the wavelength set by the grating spectrometer is the peak wavelength of the idler light.

4. Results and Discussion

Before measuring the idler light wavelength of the BGSe OPO, we used the same device that measured the idler light wavelength of KTiOAsO_4 (KTA) ($90^\circ, 0^\circ$) produced from CRYSTECH. The wavelength of the idler light was 3464 nm. In Refs. [17,18], KTA ($90^\circ, 0^\circ$) comes from the same company. Their measured data were 3467 nm and 3473 nm, respectively, and the deviation was 3 nm and 9 nm, respectively. The results showed the reliability and accuracy of the measuring devices and methods applied in this manuscript.

Then, we used BGSe to replace the KTA. When the pump energy reached 20.62 mJ, the crystal surface was slightly damaged, and the idler energy was 1.07 mJ. So, the peak wavelengths at different temperatures were measured under the pump energy of 15.74 mJ, corresponding to the idler energy of 0.62 mJ.

First, we searched and measured the output of the BGSe ($56.3^\circ, 0^\circ$) OPO in the range of 3600–3700 nm at room temperature. The oscilloscope triggered at 3611–3619 nm and failed to trigger at other wavelengths. In the experiment, the noise of the InSb detector passing through the ZAMP amplifier was slightly less than the signal of the idler light, and the oscilloscope had no data when the wavelength set by the grating spectrometer was far from the peak wavelength. So, the precise idler light output spectrum cannot be obtained, but the peak wavelength can still be measured.

As shown in Fig. 5, the output energy of BGSe ($56.3^\circ, 0^\circ$) at 3614 nm is the largest, so the peak wavelength of BGSe ($56.3^\circ, 0^\circ$) at room temperature is located at 3614 nm, which is 23 nm smaller than the theoretical value of 3637 nm. Then, we used the temperature control furnace to adjust the temperature of the BGSe crystal, recorded the peak wavelength of its idler light output at 30°C – 140°C , and compared it with the theoretical value given in Refs. [8,9].

Theoretical and experimental values are presented in Fig. 6. When the temperature of BGSe ($56.3^\circ, 0^\circ$) increased from 30°C to 140°C , the wavelength of idler frequency light under type I phase matching increased from 3637 nm to 3989 nm. The experimental values of the peak wavelength are close to the theoretical value from Ref. [9], while $\Delta\lambda_2/\Delta T$ is close to the

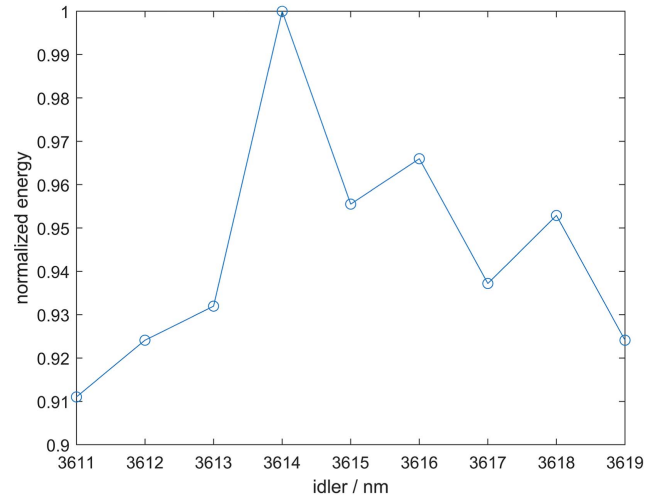


Fig. 5. Output at 3611–3619 nm of BGSe ($56.3^\circ, 0^\circ$).

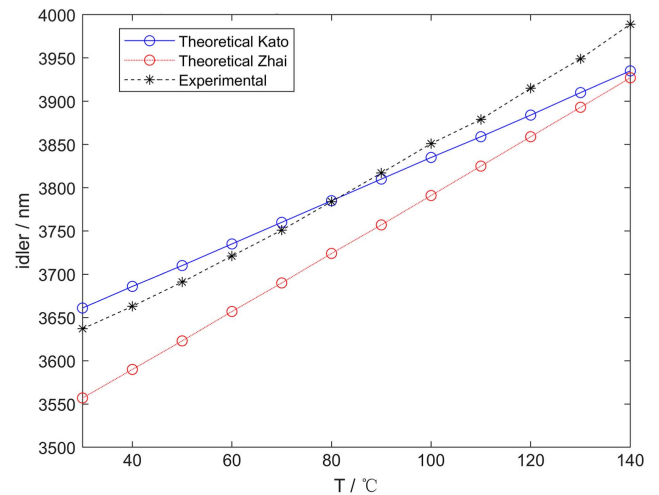


Fig. 6. Idler light's peak wavelength of BGSe ($56.3^\circ, 0^\circ$) at 30°C – 140°C .

theoretical value from Ref. [8]. $\Delta\lambda_2/\Delta T$ is 2.49 nm/ $^\circ\text{C}$ from Ref. [9], 3.36 nm/ $^\circ\text{C}$ from Ref. [8], and 3.20 nm/ $^\circ\text{C}$ from the experiment. It might be due to the experimental wavelength in Ref. [9] being wider than in Ref. [8], so the prediction of the idler wavelength is more precise. While $n_x, n_y,$ and n_z are measured directly in Ref. [8] rather than changed by SHG in Ref. [9], $\Delta\lambda_2/\Delta T$ from Ref. [8] is closer to the experimental value from this manuscript.

5. Conclusions

BGSe possesses a wide temperature tuning range. \emptyset corresponding to the maximum $\Delta\lambda_2/\Delta T$ is close to 0° when $\lambda_2 = 3 \mu\text{m}, 3.2 \mu\text{m}, 3.4 \mu\text{m}, \dots, 5 \mu\text{m}$, and $\Delta\lambda_2/\Delta T$ of type I is larger than that of type II-B. The $\Delta\lambda_2/\Delta T$ increases as λ_2 increases. When $\lambda_2 = 3 \mu\text{m}$, the maximum $\Delta\lambda_2/\Delta T = 2.358 \text{ nm}/^\circ\text{C}$; while $\lambda_2 = 5 \mu\text{m}$, the maximum $\Delta\lambda_2/\Delta T = 3.333 \text{ nm}/^\circ\text{C}$. According

to our experimental results, the wavelength of the idler light derived from Ref. [9] is more precise, while $\Delta\lambda_2/\Delta T$ derived from Ref. [8] is more precise. To the best of our knowledge, the temperature tuning of the BGSe OPO was demonstrated for the first time. The peak wavelength of the idler light is 3637 nm at 30°C and 3989 nm at 140°C, corresponding to the $\Delta\lambda_2/\Delta T$ of 3.20 nm/°C. Our results indicate that BGSe possesses advantages for application in wide band temperature tuning.

Acknowledgement

This work was supported by the Director Foundation of State Key Laboratory of Pulsed Power Laser Technology (Nos. SKL2019ZR03 and SKL2019ZR06), the Open Research Foundation of State Key Laboratory of Pulsed Power Laser Technology (No. SKL2019KF05), and the Natural Science Foundation of Anhui Province (No. 1908085MF199).

References

1. M. Q. Kang, Y. Deng, X. W. Yan, X. M. Zeng, Y. W. Guo, J. Y. Yao, F. Zeng, J. G. Zheng, K. N. Zhou, C. B. Qu, J. Q. Su, and Q. H. Zhu, "A compact and efficient 4.25 μm BaGa₄Se₇ optical parametric oscillator," *Chin. Opt. Lett.* **17**, 121402 (2019).
2. H. Y. Liu, Y. J. Yu, D. H. Sun, H. Liu, Y. H. Wang, H. Zheng, D. Li, and G. Y. Jin, "1514 nm eye-safe passively Q-switched self-optical parametric oscillator based on Nd³⁺-doped MgO:PPLN," *Chin. Opt. Lett.* **17**, 111404 (2019).
3. J. J. Song, X. H. Meng, Z. H. Wang, X. Z. Wang, W. L. Tian, J. F. Zhu, S. B. Fang, H. Teng, and Z. Y. Wei, "Harmonically pump a femtosecond optical parametric oscillator to 1.13 GHz by a femtosecond 515 nm laser," *Chin. Opt. Lett.* **18**, 033201 (2020).
4. J. Yao, D. Mei, L. Bai, Z. Lin, W. Yin, P. Fu, and Y. Wu, "BaGa₄Se₇: a new congruent-melting IR nonlinear optical material," *Inorg. Chem.* **49**, 9212 (2010).
5. J. Yao, W. Yin, K. Feng, X. Li, D. Mei, Q. Lu, Y. Ni, Z. Zhang, Z. Hu, and Y. Wu, "Growth and characterization of BaGa₄Se₇ crystal," *J. Crystal Growth* **346**, 1 (2012).
6. F. Yang, J.-Y. Yao, H.-Y. Xu, K. Feng, W.-L. Yin, F.-Q. Li, J. Yang, S.-F. Du, Q.-J. Peng, J.-Y. Zhang, D.-F. Cui, Y.-C. Wu, C.-T. Chen, and Z.-Y. Xu, "High efficiency and high peak power picosecond mid-infrared optical parametric amplifier based on BaGa₄Se₇ crystal," *Opt. Lett.* **38**, 3903 (2013).
7. N. Y. Kostyukova, A. A. Boyko, V. Badikov, D. Badikov, G. Shevyrdyaeva, V. Panyutin, G. M. Marchev, D. B. Kolker, and V. Petrov, "Widely tunable in the mid-IR BaGa₄Se₇ optical parametric oscillator pumped at 1064 nm," *Opt. Lett.* **41**, 3667 (2016).
8. N. Zhai, C. Li, B. Xu, L. Bai, J. Yao, G. Zhang, Z. Hu, and Y. Wu, "Temperature-dependent Sellmeier equations of IR nonlinear optical crystal BaGa₄Se₇," *Crystals* **7**, 62 (2017).
9. K. Kato, K. Miyata, V. V. Badikov, and V. Petrov, "Thermo-optic dispersion formula for BaGa₄Se₇," *Appl. Opt.* **57**, 2935 (2018).
10. S. J. Niu, P. Aierken, M. Ababaik, S. T. Wang, and T. Yusufu, "Widely tunable, high-energy, mid-infrared (2.2–4.8 μm) laser based on a multi-grating MgO:PPLN optical parametric oscillator," *Inf. Phys. Technol.* **104**, 103121 (2020).
11. V. Badikov, D. Badikov, G. Shevyrdyaeva, A. Tyazhev, G. Marchev, V. Panyutin, V. Petrov, and A. Kwasniewski, "Phase-matching properties of BaGa₄S₇ and BaGa₄Se₇: wide-bandgap nonlinear crystals for the mid-infrared," *Phys. Status Solidi RRL* **5**, 31 (2011).
12. F. Yang, J. Yao, H. Xu, F. Zhang, N. Zhai, Z. Lin, N. Zong, Q. Peng, J. Zhang, D. Cui, Y. Wu, C. Chen, and Z. Xu, "Midinfrared optical parametric amplifier with 6.4–11 μm range based on BaGa₄Se₇," *IEEE Photon. Technol. Lett.* **27**, 1100 (2015).
13. E. Boursier, P. Segonds, B. Ménaert, V. Badikov, V. Panyutin, D. Badikov, V. Petrov, and B. Boulanger, "Phase-matching directions and refined Sellmeier equations of the monoclinic acentric crystal BaGa₄Se₇," *Opt. Lett.* **41**, 2731 (2016).
14. K. Kato, K. Miyata, and V. Petrov, "Phase-matching properties of BaGa₄Se₇ for SHG and SFG in the 0.901–10.5910 μm range," *Appl. Opt.* **56**, 2978 (2017).
15. W.-Q. Zhang, "General ray-tracing formulas for crystal," *Appl. Opt.* **31**, 7328 (1992).
16. H. Kong, J. T. Bian, and X. Q. Sun, "Calculation of phase-matching angles and effective nonlinear coefficients of BaGa₄Se₇ crystals," *Optik* **193**, 163004 (2019).
17. F. Bai, "The studies of novel solid-state lasers based on optical parametric oscillation and stimulated Raman scattering," Ph.D thesis (Shandong University, 2013).
18. X. Dong, "All-solid-state KTA optical parametric oscillation," Master thesis (Shandong University, 2009).